Carbohydrate Polymers 97 (2013) 864–867

Contents lists available at SciVerse ScienceDirect

Carbohydrate Polymers

journal homepage: www.elsevier.com/locate/carbpol

Corrigendum

Corrigendum to "Structure of arabinogalactan-protein from Acacia gum: From porous ellipsoids to supramolecular architectures" [Carbohydr. Polym. 90 (2012) 322–332]

D. Renard[a,*], C. Garnier[b], A. Lapp[c], C. Schmitt[d], C. Sanchez[e]

[a] INRA, UR1268 Biopolymères Interactions Assemblages, F-44300 Nantes, France
[b] UMR CNRS 6290 Equipe TAF «Translation and Folding», Université de Rennes 1, Campus Beaulieu, F-35042 Rennes cedex, France
[c] Laboratoire Léon Brillouin, CEA Saclay, Bâtiment 563, F-91191 Gif-sur-Yvette, France
[d] Department of Food Science and Technology, Nestlé Research Center, Vers-chez-les-Blanc, CH-1000 Lausanne 26, Switzerland
[e] UMR1208 Ingénierie des Agropolymères et Technologies Emergentes, INRA-Montpellier SupAgro-CIRAD-Université Montpellier 2, Place Pierre Viala, F-34060 Montpellier, France

Dear Editor,

We wish to report a problem with the TEM images in our previously published paper *Structure of arabinogalactan-protein from Acacia gum: From porous ellipsoids to supramolecular architectures*. Indeed, we clearly identified some pollutants from the rinsing fluid used to wash carbon grids for TEM observations. The origin of the pollutant was unknown (salt, colloid, other) but we were convinced that cross-contamination between AGP samples and this pollutant during grids preparation was at the origin of AGP self-association leading to false structures we observed by microscopy and published in the manuscript. These conclusions came from new TEM observations performed by Eléonore Lepvrier (UMR CNRS 6290 Equipe TAF "Translation and Folding", Université de Rennes) on two different instruments (Jeol 120 kV or FEI Tecnai 200 kV microscope). The new TEM observations using two different techniques of samples preparation (samples were either applied on carbon-coated copper grids either sprayed on grids) clearly demonstrated that large objects with dimensions of about 100 nm and up to 200 nm were never present on grids leading to the conclusion that previous TEM observations were not in agreement with single AGP macromolecules observations but came from AGP self-association due to the presence of pollutants. In addition, the polyelectrolyte character of AGP from Acacia gum could reinforce the formation of false aggregated structures due to interactions between AGP macromolecules and the pollutant. Figs. 5–7 show the correct images and these should replace Figs. 5–8 in the original paper.

The new TEM images affected accordingly the main conclusions regarding the structural details of AGP from Acacia gum as follows.

It is first important to notice that imaging AGP structures is far from being a trivial task. This difficulty probably explains that very few micrographs of AGP were published in the past. The main difficulty arises from the remarkable surface properties of AGP that render the observation of single macromolecules a very hard work. It is therefore common to observe a continuous thin film on the carbon grids without any visible individual structures. To partly overcome this limitation, different samples preparation for TEM observations varying the method of sample deposition onto the carbon grid (either by simple deposition either by spraying of the sample drop onto the grid), and different AGP concentrations, were tested. TEM micrographs were also obtained using three different microscopes (Jeol, Tecnai™ and Philips). All the micrographs we obtained revealed basically the same structural organization of AGP with some differences in individual AGP density depending on the samples preparation and AGP concentration used. An alternative to these limitations was the use of cryo-TEM in order to maintain the sample in a hydrated form and therefore decrease the strong adhesion on grids. Preliminary cryo-TEM observations made on AGP samples were difficult to analyse due to the very low electronic contrast of the observed structures. Nevertheless, the morphological aspects of the structures were in agreement with those observed using TEM.

Two TEM micrographs (a, b) at two magnifications are shown in Fig. 5. These two micrographs were carefully selected and were representative of all the images (about 60) we observed. The first remark was that highly contrasted isolated particles (foreground) were visible besides less contrasted particles that were organized in a kind of network (background). The shape of isolated particles was either spheroidal (Fig. 5a, a1) either more anisotropic (Fig. 5b, b1). A distribution of sizes was clearly apparent within each class of particles. Spheroidal particles displayed diameters ranging from about 10 to 40 nm while anisotropic particles displayed lengths from 20 up to about 60 nm. It can be noticed here that the maximum particle dimension determined from the $P(r)$ function by SANS was 64 nm (see Fig. 4). The second important remark was that both spheroidal and more elongated particles were apparently constituted of smaller structural subunits (Fig. 5a1, b1). At these

DOI of original article: http://dx.doi.org/10.1016/j.carbpol.2012.05.046.
* Corresponding author. Tel.: +33 2 40 67 50 52; fax: +33 2 40 67 50 25.
E-mail address: denis.renard@nantes.inra.fr (D. Renard).

http://dx.doi.org/10.1016/j.carbpol.2013.05.006

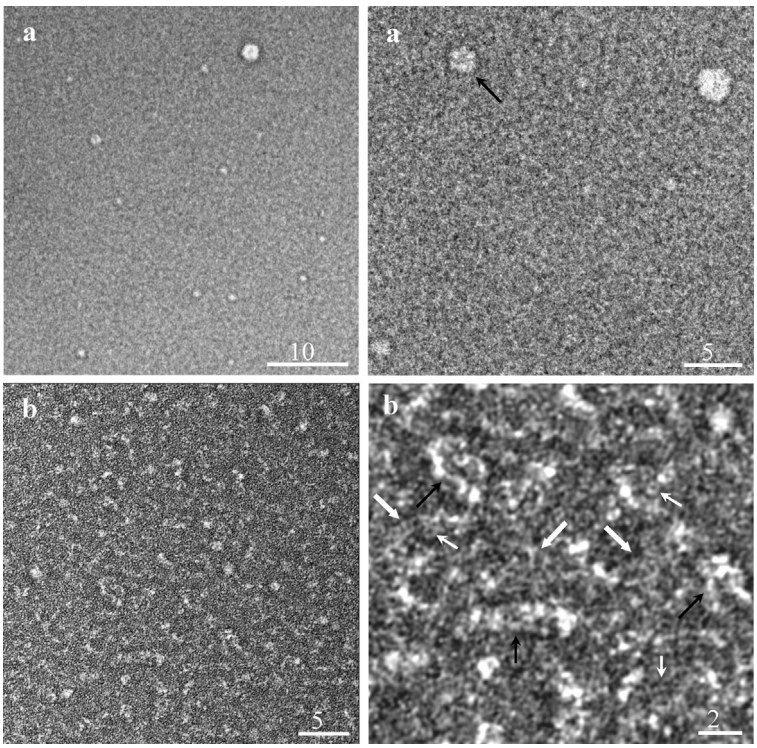

Fig. 5. TEM micrographs at two magnifications of arabinogalactan-protein (AGP) from Acacia gum dispersed at 1 wt% in 50 mM NaCl; (a1) (b1) magnifications of (a) and (b), respectively. Black thin arrows show examples of particles composed by structural subunits. Thick white arrows show linear and branched chains. Thin white arrows show ring-like structures.

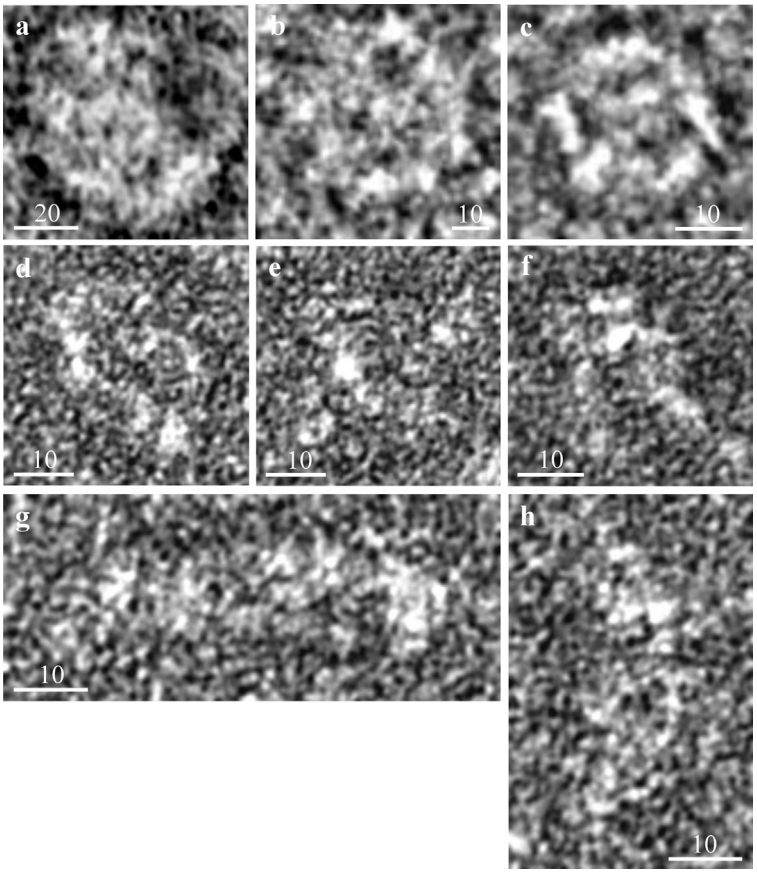

Fig. 6. Structural details of eight particles (a–h) captured from TEM micrographs of arabinogalactan-protein (AGP) from Acacia gum dispersed at 1 wt% in 50 mM NaCl. After capturing one particle from raw micrographs such as those shown in Fig. 5, image contrast was changed when necessary and images were filtered using a bandpass FFT filter. An additional filtering was then made using the CLAE (Contrast Limited Adaptive Histogram Equalization) ImageJ plugin.

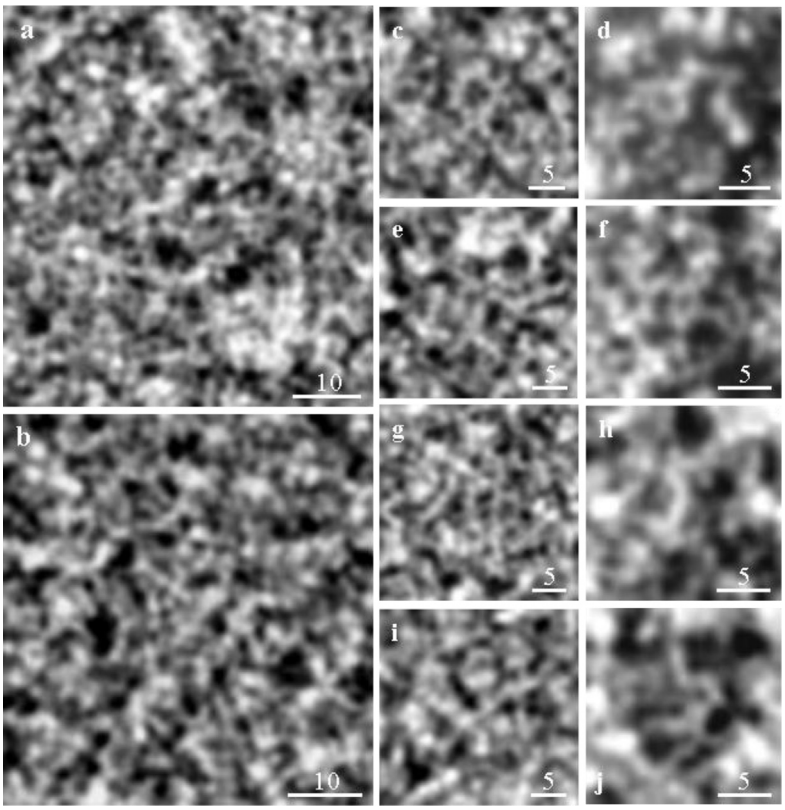

Fig. 7. Structural details at high resolution of TEM micrographs background. Image analyses were performed as those in Fig. 6. Note the remarkable likeness of the structure in Fig. 7i with the wattle-blossom model.

magnifications, the background was more difficult to describe as the grid was fully covered by AGP, but we can observe in Fig. 5b1 entangled linear and branched chains and a significant amount of ring-like structures.

Since the micrographs we have described were obtained by scanning negative films at high resolution (about 1 nm for 3 pixels), it was possible at this scale to observe for the first time the finest details of AGP structures. Typical examples of results obtained are shown in Fig. 6, with smaller objects (Fig. 6a–c) appearing more spherical than larger ones that were somewhat more elongated (Fig. 6d–h). An interesting feature of some spheroidal particle morphologies was the presence of an outer structure combined to an inner porous network of interspersed chains or interacting structural blocks (Fig. 6b,c). The same kind of structural organization ("3D organization") was demonstrated for the arabinogalactan (AG) fraction of Acacia gum (Sanchez et al., 2008). It is then possible that the particles in Fig. 6b and c could be AG eluted with the AGP fraction during fractionation by hydrophobic interaction chromatography. Remarkably, all the particles were porous supramolecular assemblies of smaller structural subunits with dimensions of about 2–10 nm. These building structural subunits were mainly branched chains and ring-like structures with diameters of about 1–5 nm. It is important to note that a huge number of ring-like structures were observed in all micrographs we studied. These ring-like structures were also observed in cryo-TEM images, emphasizing the absence of artefacts due to dehydration process mandatory for TEM observations. Interestingly, ring-like structures formed from interacting hydroxyproline-rich glycoproteins, with dimensions however much larger than those measured in our study, have been shown by atomic force microscopy (Wegenhart et al., 2006). The ring-like structures with dimensions in the 1–5 nm range we identified would be much more in agreement with the ring-like structure of the galactan backbone calculated by molecular modelling in a Hyp-AG subunit consisting of 15-sugar residues attached to one hydroxyproline (Lamport and Várnai, 2013). In addition, the high conformational flexibility of this glycomotif could be efficiently stabilized by intramolecular binding with calcium ions due to the presence of two side chains glucuronic acid residues (Lamport and Várnai, 2013). As suggested by the authors, these structural features obtained on a small arabinogalactan-peptide could be conserved on larger Hyp-AGs.

Finally, we described in more details micrograph backgrounds that were in fact a highly porous network of surface-active AGP adsorbed onto the grids (Fig. 7). A careful observation of micrographs allowed the extraction of some interesting structural organization features of AGP (Fig. 7a, b). It was clear that interacting branched chains, aggregated chains and ring-like structures were mostly present. The numerous branched chains and branched ring-like structures identified in the background of AGP TEM images could be due to the self-association of the highly flexible Hyp-AG glycomodules forming a sort of interspersed network of branched chains and rings. These different structures were magnified in Fig. 7c–j. One can see for instance in Fig. 7c, d, j branched rings with diameters of 3–5 nm. Fig. 7c clearly showed a branched ring connected to a more linear chain. Entangled chains forming aggregates were also visible in Fig. 7e–g. Probably the most surprising picture we obtained is Fig. 7i where a linear chain with branched building blocks can be observed. Such a structure closely looks like the famous wattle-blossom model so many times hypothetically described in the literature as the structure of AGP from Acacia gum.

The presence of both isolated AGP assemblies and a surface film of entangled chains and small aggregates question on why all the structures did not form a film. One possibility is that large supramolecular structures diffuse more slowly to the solid–liquid interface created by the droplet onto the grid than less organized AGP, then appeared in the foreground. Alternatively, larger

structures could be less surface-active than single AGP. Anyway, it was not possible from micrographs to conclude on the whole morphology of adsorbed AGP even whether SANS data suggested an ellipsoidal morphology in solution.

Supplemental references

Wegenhart, B., Tan, L., Held, M., Kieliszewski, M. J., & Chen, L. (2006). Aggregate structure of hydroxyproline-rich glycoprotein (HRGP) and HRGP dispersion of carbon nanotubes. *Nanoscale Research Letters, 1*, 154–159.

Lamport, D. T. A., & Várnai, P. (2013). Periplasmic arabinogalactan glycoproteins act as a calcium capacitor that regulates plant growth and development. *New Phytologist, 197*, 58–64.

Sincerely yours

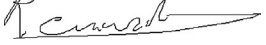

Dr Denis Renard